The Astrophysical Journal, 574:861–872, 2002 August 1

COLLECTIVE PROCESSES IN RELATIVISTIC PLASMA AND THEIR IMPLICATIONS FOR GAMMA-RAY BURST AFTERGLOWS

Amir Sagiv and Eli Waxman
Department of Condensed Matter Physics, Weizmann Institute, Rehovot 76100, Israel;
amir@wicc.weizmann.ac.il, waxman@wicc.weizmann.ac.il
Received 2002 February 18; accepted 2002 March 31

ABSTRACT

We consider the effects of collective plasma processes on synchrotron emission from highly relativistic electrons. We find, in agreement with the 1970 work of Sazonov, that strong effects are also possible in the absence of a nonrelativistic plasma component, due to the relativistic electrons (and protons) themselves. In contrast with Sazonov, who infers strong effects only in cases in which the ratio of plasma frequency to cyclotron frequency is much larger than the square of the characteristic electron Lorentz factor, $\nu_p/\nu_B \gg \gamma_e^2$, we also find strong effects for $1 \ll \nu_p/\nu_B \ll \gamma_e^2$. The modification of the spectrum is prominent at frequencies $\nu \le \nu_{R*} \equiv \nu_p \min\{\gamma_e, (\nu_p/\nu_B)^{1/2}\}$, where ν_{R*} generalizes the "Razin-Tsytovich" frequency $\nu_R \equiv \gamma_e \nu_p$ to the regime $\nu_p/\nu_B \ll \gamma_e^2$. Applying our results to gamma-ray burst (GRB) plasmas, we predict a strong modification of the radio spectrum on a minute timescale following the GRB at the onset of fireball interaction with its surrounding medium, in cases in which the ratio of the energy carried by the relativistic electrons to the energy carried by the magnetic field exceeds $\sim 10^5$. Plausible electron distribution functions may lead to negative synchrotron reabsorption, i.e., to coherent radio emission, which is characterized by a low degree of circular polarization. Detection of these effects would constrain the fraction of energy in the magnetic field, which is currently poorly determined by observations, and moreover would provide a novel handle on the properties of the environment into which the fireball expands.

Subject headings: gamma rays: bursts — masers — plasmas — radiation mechanisms: nonthermal — radio continuum: general

1. INTRODUCTION

According to the model now prevailing (see Piran 2000; Mészáros 2002 for recent reviews), gamma-ray bursts (GRBs) originate from the dissipation of the kinetic energy of a relativistically expanding fireball, caused by a cataclysmic collapse of a massive star or by a neutron star–neutron star (NS-NS) or neutron star–black hole (NS-BH) merger event, leading to the acceleration of a plasma of electrons and protons to highly relativistic speed. Part of the kinetic energy of this expanding "fireball" is dissipated in "internal" collisions between different parts of the inhomogeneous ejecta, resulting in shocks that accelerate particles via the Fermi process to ultrarelativistic energies. The nonthermal radiation from accelerated electrons reproduces well the observed MeV gamma-ray spectra. At a later stage of the expansion, the fireball decelerates because of interaction with its surrounding medium. The relativistic shock wave driven into the ambient medium continuously accelerates new electrons of the surrounding gas, producing a long-term synchrotron "afterglow" emission.

Although observations are in general agreement with model predictions (see Kulkarni et al. 2000 for a recent review), the model is incomplete, and there are several open issues that are not properly understood. One is that of the burst progenitor. Several alternative models for the "inner engine" were suggested, such as an NS-NS or NS-BH merger (Paczyński 1986; Goodman 1986) and the gravitational collapse of massive stars (Woosley 1993; Paczyński 1998; MacFadyen & Woosley 1999). Unfortunately, at present neither GRB nor afterglow observations provide decisive evidence in support of a particular model. Nevertheless, the environment may be a clue to the progenitor. Thus, expansion into a relatively uniform interstellar medium (ISM) with a number density $n \sim 1$ cm^{-3} would be a natural consequence of a "merger" scenario, whereas if the progenitor is a collapsing star, it is natural to expect a much higher ambient density due to a wind ejected by the star at earlier stages of its evolution. The "onset" of fireball interaction with the surrounding medium, i.e., at the radius where fireball deceleration becomes significant, typically takes place on a minute timescale (in the observer frame) following the burst, at which stage the density of the wind plasma is $n \sim 10^4$ cm^{-3}. At present, afterglow observations typically begin several hours following the burst and do not allow a direct probe of the onset of deceleration. Since on a day timescale the fireball expands to the point where the wind density drops to values close to that typical for the ISM, present observations do not provide clear discriminants between the wind and ISM scenarios (Livio & Waxman 2000).

A second issue in which basic understanding is still lacking is the physics of acceleration of electrons to high energies and the buildup of strong magnetic fields by the GRB collisionless shock waves (Gruzinov & Waxman 1999). The presence of high-energy electrons and strong magnetic fields is implied by observations, yet there is currently no theory based on first principles that satisfactorily explains electron coupling and magnetic-field generation. The ignorance is usually parameterized by two dimensionless parameters ξ_e and ξ_B, which stand for the fractions of shock internal energy density that are carried by the relativistic electrons and by the magnetic field, respectively. Efforts to constrain these parameters using afterglow observations are numerous, and ξ_e is typically estimated to be close to its equipartition value, i.e., $\xi_e \sim \frac{1}{3}$. However, ξ_B is not well constrained

by observations, and its estimated values range from $\xi_B \sim 10^{-1}$ (e.g., Waxman 1997a; Wijers & Galama 1999) to $\xi_B \sim 10^{-6}$ (e.g., Wijers & Galama 1999; Chevalier & Li 1999; Galama et al. 1999; Waxman & Loeb 1999).

Observations strongly suggest that the radiation emitted during the afterglow is synchrotron radiation. We show here that the modification of the refractive index by the relativistic electrons and protons may strongly affect the emission at radio wavelengths during the onset of fireball deceleration, if $\xi_B \ll 1$. Moreover, we find that under plausible assumptions about the electron distribution function, the synchrotron reabsorption coefficient may become negative, thus leading to coherent emission from the fireball on a minute timescale following the GRB. These collective plasma processes strongly affect the synchrotron spectrum at frequencies $\leq \nu_{R*} = \nu_p(\nu_p/\nu_B)^{1/2}$, where $\nu_p/\nu_B \sim (\xi_e/\xi_B)^{1/2}$ is the ratio of the plasma frequency and the electron gyration frequency.

As mentioned above, currently there is a few hours gap between GRB and afterglow observations. However, the (operating) *High Energy Transient Explorer 2* (*HETE-2*) satellite and the *Swift* satellite (planned to be launched in 2003) may allow observations of early stages of fireball expansion shortly after the GRB, thus providing data on the onset of deceleration. We show below that future observations of collective plasma effects in the emission from GRB afterglows will serve to constrain the value of ξ_B, as well as the parameters of the environment into which the fireball expands, thus providing a handle on both progenitor type and shock physics.

Collective plasma effects on synchrotron emission and reabsorption have been considered by many authors (e.g., Ginzburg & Syrovatskii 1965; Zheleznyakov 1967; Yokun 1968; Crusius & Schlickeiser 1988). Analyses of effects due to a nonvacuum index of refraction are typically limited to the case in which the index of refraction is determined by the presence of a nonrelativistic plasma. These analyses do not apply to the GRB plasma in which we are interested, in which no "cold" nonrelativistic plasma component is present. Sazonov (1969, 1970, 1973) has studied the case of interest for us, in which "cold" plasma is absent, and the effects are entirely due to the presence of the relativistic plasma. As we show below, his results are too restrictive, as he infers negative reabsorption only in cases in which $\nu_p/\nu_B \gg \gamma_e^2$, or in cases in which the electron distribution function is very anisotropic. We find that these constraints might be eased and that negative reabsorption is possible for isotropic distribution functions provided that $\nu_p \gg \nu_B$, thus allowing coherent emission for GRB plasma parameters.

In § 2 we derive the dispersion relation and the polarizations and refractive indices of normal modes in a highly relativistic, weakly magnetized ($\nu_p/\nu_B \gg 1$) plasma with isotropic electron and proton distribution functions. The frequency range discussed is $\nu_p < \nu \ll \gamma_e \nu_p \equiv \nu_R$, in which the relativistic plasma may have a strong effect on synchrotron emission. In § 3 we show that the plasma strongly affects synchrotron radiation at frequencies $\nu \leq \nu_{R*} = \nu_p(\nu_p/\nu_B)^{1/2}$, which generalizes the Razin-Tsytovich frequency ν_R to a regime in which $(p/\nu_B)^{1/2} \ll \gamma_e$—the regime relevant for us. We note that although ν_R is commonly quoted as the frequency below which plasma effects are strong, it is typically found in numerical analyses of nonrelativistic plasmas that for $\nu_p/\nu_B \gg 1$, synchrotron emission is strongly modified only at $\nu \leq \nu_{R*}$ (e.g., Crusius & Schlickeiser 1988). We show in § 3 that a more careful statement of the qualitative criterion, which leads to the conclusion that plasma effects are strong below ν_R (e.g., Rybicki & Lightman 1979, § 8.3), leads directly to the result that (for both relativistic and nonrelativistic plasma) such effects are important only below ν_{R*}.

Our results are applied to GRB plasmas in § 4. In § 4.1 we briefly describe GRB and afterglow phenomenology, give a short review of the fireball model, and derive the plasma parameters during the onset of fireball deceleration, considering both expansion into a uniform-density ISM (§ 4.1.1) and expansion into a wind (§ 4.1.2). Plasma effects are discussed in § 4.2. The implications of our results are discussed in § 5.

We note that coherent radio emission from GRBs has recently been discussed by Usov & Katz (2000). The scenario considered by these authors for GRB production, the scattering of ambient-medium electrons and protons by a magnetically dominated wind (Smolsky & Usov 2000), is different, however, from the scenario we are considering, in which observed radiation is produced (in both GRB and afterglow phases) by the dissipation through collisionless shocks of fireball kinetic energy, leading to magnetic-field amplification and to particle acceleration. The processes we consider are thus different from those considered by Usov & Katz (2000), and the predicted radio emission is very different. For example, while Usov & Katz (2000) find a power-law spectrum with strong emission at less than 1 MHz for a strong magnetic field, we find strong emission only for weak magnetic fields and over a narrow range of frequencies around ~0.1 GHz (which is more readily observable).

Finally, we note that the analysis presented here is restricted to isotropic electron and proton distributions, and we show that strong plasma effects on synchrotron radiation occur if $\nu_p \gg \nu_B$. We note, however, that anisotropy may lead to further interesting effects, the discussion of which is beyond the scope of this work.

2. WAVES IN A WEAKLY MAGNETIZED RELATIVISTIC PLASMA WITH ISOTROPIC ELECTRON AND PROTON DISTRIBUTION FUNCTIONS

As explained in the next section, it is the deviation of the speed at which light propagates in plasma from c that is responsible for the plasma effects we consider. This implies that we must first obtain expressions for the refractive indices $n_{1,2}(\omega)$ of the transverse electromagnetic modes in the plasma. In our derivation of the dispersion relation, we restrict the discussion to plasmas under the following conditions: (1) highly relativistic electrons; (2) a rough energy equipartition between protons and electrons; (3) isotropic particle distribution functions; and (4) weak magnetization, $\nu_p/\nu_B \gg 1$. Afterglow observations imply that conditions 1 and 2 hold for GRB plasmas. Condition 3 restricts the discussion to plasma effects originating from the deviation of the refracting indices from their vacuum values. Our discussion is restricted to the weak magnetization case, since as shown in the next section, strong effects of the plasma on synchrotron emission are obtained for this case only. Finally, we restrict the discussion to the frequency range affected by collective effects, $\nu_B \ll \nu_p < \nu \ll \gamma_e \nu_p$.

The assumption $\nu_p/\nu_B \gg 1$ allows a perturbative derivation (in ν_B/ν_p) of the dispersion relation. Moreover, in the

frequency range $\nu_B \ll \nu_p < \nu \ll \gamma_e \nu_p$, the deviation of the refractive index $n = kc/\omega$ from 1 is much larger than $1/\gamma_e^2$. This simplifies the dispersion relations obtained below, thus allowing analytic estimates. Below we give order-of-magnitude estimates of the plasma frequency and the difference between the refractive indices of the transverse electro magnetic waves in a relativistic plasma. Exact calculations are given in the Appendix and are used to verify the simple estimates.

As we show in § A1, the refractive indices of the transverse electromagnetic waves in a field-free plasma are degenerate and approximately satisfy the relation

$$n^2(\nu) = 1 - \frac{\nu_p^2}{\nu^2} \ ,$$
$$\nu_p = \frac{1}{2\pi}\left(\frac{4\pi n_e e^2}{\gamma_{e0} m_e} + \frac{4\pi n_p e^2}{\gamma_{p0} m_p}\right)^{1/2} \ , \qquad (1)$$

where ν_p is the plasma frequency of a relativistic plasma. This result is exact for monoenergetic electron and proton distributions, where γ_{e0} and γ_{p0} are the associated Lorentz factors of the two species, respectively. Detailed calculations show, however, that the above result is also a good approximation to the plasma frequency for more general energy distributions. For a power-law energy distribution implied by afterglow observations, $n(\gamma) \propto \gamma^{-2}$ for $\gamma > \gamma_{\rm min}$, replacing γ_0 with $\gamma_{\rm min}$ in equation (1) gives the plasma frequency with an accuracy of 1%. Note that equation (1) is a natural generalization to the relativistic regime of the familiar expression for the plasma frequency, obtained by replacing the particle mass m with γm. Since we assume that the energy of the electrons and protons is approximately equipartitioned, the contributions of the two species to ν_p are comparable.

Once an external magnetic field $\boldsymbol{B}_0$ is introduced, the plasma cannot be regarded as isotropic any longer, and the degeneracy of the two refractive indices is removed. For frequencies $\nu \ll \nu_B$, the effect of the magnetized plasma on the propagating radiation is small, and the electric field can be assumed to be approximately transverse to the direction of propagation, i.e., $\boldsymbol{E} \perp \boldsymbol{k}$. In the Appendix (§ A2) we derive the dispersion relation for the waves of a transverse electric field. In order to obtain estimates of the refractive indices of the transverse electromagnetic modes, we solve the Vlasov equation of a relativistic plasma with isotropic electron and proton distribution functions. The assumption of weak magnetization allows a perturbative expansion of the equation, where the perturbations in the particle distribution functions are assumed to be linear in the external magnetic field (i.e., the expansion parameter is ν_B/ν_p). This leads to a significant simplification of the formalism. The dispersion relation for the components of the transverse electric fields is given by

$$\frac{k^2 c^2}{\omega^2} E_i = \epsilon_{ij} E_j \quad \text{with} \quad i,\ j = 1,\ 2 \ , \qquad (2)$$

where $\omega = 2\pi\nu$ is the radian frequency of the wave, k is the wavenumber, and ϵ_{ij} is the 2×2 dielectric tensor. The refractive indices $n_{1,2}(\omega) = ck_{1,2}/\omega$ of the plasma are the square roots of the eigenvalues of this equation. Detailed numerical calculations showed that the values obtained for the components of the dielectric tensor and the resulting refractive indices are not sensitive to the exact shape of the electron and proton energy distribution functions. Specifically, we showed that simple expressions obtained for monoenergetic distribution functions (which are the estimates used below) are good approximations of the more cumbersome expressions obtained for power-law distributions.

The deviation from degeneracy of the two refractive indices is the consequence of the nondiagonal terms of the dielectric tensor, which are proportional to $\cos\phi$, where ϕ is the angle between the wavevector $\boldsymbol{k}$ and the external magnetic field $\boldsymbol{B}_0$ (eqs. [A5a] and [A9]). Hence, the deviation is largest for radiation propagating along the magnetic field ($\phi = 0$) and vanishes when the direction of propagation is perpendicular to the magnetic field ($\phi = \pi/2$). Equations (A6) and (A10), describing the diagonal and off-diagonal elements of the dielectric tensor, can be used to estimate the difference between the two refractive indices. For the frequencies in which we are interested, $1 - n$ is larger than, or at least comparable to, $1/\gamma_{e,p}^2$. This simplifies the algebra immensely. Since we assume that the widths of the electron and proton distribution functions are close and that energy density in the protons and electrons is approximately equipartitioned, the contributions of the two species to $\Delta n = n_1 - n_2$ are comparable. Hence, an order-of-magnitude estimate of Δn is

$$\Delta n \sim \frac{\nu_p^2 \nu_B}{\nu^3} \cos\phi \ln\left(\frac{\nu_p^2}{4\nu^2}\right) \ , \qquad (3)$$

up to a factor of the order of 1.

The result $\Delta n_{\phi=\pi/2} = 0$ is a consequence of the fact that our derivation only keeps terms that are linear in the magnetic field, i.e., first-order terms in ν_B/ν_p. If this assumption is eased and the refractive indices of the ordinary and extraordinary modes are used to estimate $\Delta n_{\phi=\pi/2}$, we obtain $\Delta n_{\phi=\pi/2} = (1/2)(\nu_B/\nu)^2(1 - \nu_p^2/2\nu^2)$. As is shown in the next section, the frequency at which the plasma has a significant effect on the synchrotron emission is $\nu_{\rm R}* = \nu_p(\nu_p/\nu_B)^{1/2}$. This implies that for plasma parameters of interest to us ($\nu_p/\nu_B \lesssim 10^3$), the logarithmic factor in equation (3) is of the order of 10. Hence, we replace equation (3) with an expression that takes into account the finite Δn at perpendicular propagation

$$\Delta n(\phi) \simeq \begin{cases} \dfrac{\nu_p^2 \nu_B}{\nu^3} \cos\phi \ln\left(\dfrac{\nu_p^2}{4\nu^2}\right) \ , & \left|\dfrac{\pi}{2} - \phi\right| > \dfrac{1}{10}\dfrac{\nu_B \nu}{\nu_p^2} \ , \\ \dfrac{1}{2}\dfrac{\nu_B^2}{\nu^2}\left(1 - \dfrac{\nu_p^2}{2\nu^2}\right) \ , & \text{otherwise} \ . \end{cases} \qquad (4)$$

We solved the dispersion relation (eqs. [A6] and [A10]) numerically for two values of γ_e (920 and 4.6×10^4) and for three values of ν_B/ν_p (10^{-1}, 10^{-2}, and 10^{-3}). These values of γ_e and ν_B/ν_p are representative of typical values for GRB afterglow plasmas (see § 4). In these calculations, we assumed a propagation angle $\phi = \pi/4$. The results agree with the estimate in equation (4) up to a factor of $\sim$2. The numerical calculation also confirmed that for parameters in the ranges relevant for GRB afterglows, the discrepancy between the refractive indices of the transverse modes is small in comparison to the deviation of either of them from unity, i.e., $|n_1 - n_2| \ll (1 - n_{1,2})$.

When the radiation propagates parallel to the magnetic field, the squared refractive indices of the two normal modes

can be described by the well-known expressions

$$\epsilon_R = 1 - \frac{\nu_{pe}^2}{\nu(\nu - \nu_{Be})} - \frac{\nu_{pp}^2}{\nu(\nu + \nu_{Bp})} ,$$
$$\epsilon_L = 1 - \frac{\nu_{pe}^2}{\nu(\nu + \nu_{Be})} - \frac{\nu_{pp}^2}{\nu(\nu - \nu_{Bp})} , \quad (5)$$

where ν_{Be} and ν_{Bp} are the gyration frequencies of electrons and protons in the magnetic field and ν_{pe} and ν_{pp} are the relativistic plasma frequencies of the two species, respectively. It is instructive to compare our estimate in equation (4) with the difference $n_R - n_L$ obtained from equation (5). When exact equipartition is assumed and both the protons and the electrons are monoenergetically distributed, $\nu_{pe} = \nu_{pp} = \nu_p$ and $\nu_{Be} = \nu_{Bp} = \nu_B$, whence $\epsilon_R = \epsilon_L = 1 - 2\nu_p^2/(\nu^2 - \nu_B^2)$. This degeneracy is removed if equipartition is not exactly satisfied or if the widths of the distribution functions of the two species are different. Since both effects are expected to be important in the case of our interest, we use equation (4) as an estimate for Δn.

Our calculations imply that nondiagonal elements of the dielectric tensor are smaller than its diagonal elements by a factor of the order of $\nu_B/\nu \ll 1$. The latter, however, are independent of the magnetic field and thus are identical to the values we obtained for a field-free plasma (see eq. [A5a]). As is discussed in § 3, the difference between the refractive indices of the transverse modes is important for determining the polarization of the modes and thus for the calculation of synchrotron self-absorption. However, our estimate of the frequency at which plasma effects on synchrotron emission become significant is not sensitive to Δn. Therefore, as far as estimating the frequency $\nu_{R*} = \nu_p(\nu_p/\nu_B)^{1/2}$ is concerned, we use the approximation given in equation (1).

The detailed expressions we obtained (in the Appendix) for the elements of the 2×2 dielectric tensor ϵ_{ij} show that $\epsilon_{11} = \epsilon_{22}$ and $\epsilon_{12} = -\epsilon_{21}$ (see eqs. [A6] and [A10]). The assumption of transversality thus implies that the normal modes are always circularly polarized (clockwise and counterclockwise). To check the consistency of our assumption of quasi transversality and to obtain the (elliptical) polarization of the two quasi-transverse modes, we calculated the eigenmodes of the full 3×3 dielectric tensor. Following the method outlined in § A1 (and described in the paragraph preceding eq. [2]), it is straightforward (yet lengthy) to obtain expressions for the other elements of ϵ_{ij} with $i, j = 1$, 2, 3 and *without* assuming transversality. It is possible to show that these extra elements contribute an additional term to Δn, which is smaller than the value obtained from the transverse calculation by a factor of $\sim 0.1(\ln|\nu_B/4\nu_p|)^{-4}\nu_p/\nu_B \sim 10^{-2}$ at small and mildly oblique propagation angles and becomes comparable to $(1/2)(\nu_B^2/\nu^2)[1 - (\nu_p^2/2\nu^2)]$ as $|\pi/2 - \phi|$ approaches $0.1\nu_B\nu/\nu_p^2$. Numerical calculation of the plasma normal modes confirmed that for plasma parameters of interest to us ($\gamma_e = 10^3$–10^4, $\nu_p/\nu_B = 10^2$–10^3), the normal modes are indeed transverse to the direction of propagation and are left- and right-circularly polarized.

3. EFFECTS ON SYNCHROTRON EMISSION

The spectral characteristics of synchrotron emission by a single relativistic electron are determined by the beaming of the radiation emitted by the electron into a narrow cone about the instantaneous direction of the electron's motion. When the electron is in a vacuum, the opening angle of this cone depends on the electron's Lorentz factor and the frequency of the radiation. Three regimes should be considered: When the frequency of interest is higher than the characteristic synchrotron frequency ν_c, the cone's opening angle is $\Delta\theta \simeq (\nu_c/\nu)^{1/2}/\gamma$, and $\nu \sim \nu_c$, one obtains the familiar result $\Delta\theta \simeq 1/\gamma$; If, however, the frequency of interest is much smaller than ν_c, one obtains $\Delta\theta \simeq (\nu_c/\nu)^{1/3}/\gamma$. Next we consider an electron that is embedded in a dielectric medium with a refractive index $n \neq 1$. Since the speed of light is now c/n, the opening angle of the cone is $\Delta\theta \simeq [(\nu_c/\nu)(1/\gamma^2) + 1 - n^2(\nu)]^{1/2}$ for $\nu > \nu_c$, $\Delta\theta \simeq [1/\gamma^2 + 1 - n^2(\nu)]^{1/2}$ for frequencies $\nu \sim \nu_c$, and $\Delta\theta \simeq [(\nu_c/\nu)^{2/3}(1/\gamma^2) + 1 - n^2(\nu)]^{1/2}$ for frequencies much smaller than ν_c. When the dielectric medium is a plasma, we use $1 - n^2 = \nu_p^2/\nu^2$. A strong deviation from vacuum behavior occurs when the second term $(\nu_p/\nu)^2$ is comparable to the first term in the square brackets. Using $\nu_c = \gamma^3\nu_B$, where ν_B is the gyration frequency of the electron, we obtain an expression for the frequency at which the collective plasma effects greatly influence the synchrotron emission:

$$\nu_{R*} \simeq \nu_p \min\left\{\gamma, \sqrt{\frac{\nu_p}{\nu_B}}\right\} . \quad (6)$$

The Razin-Tsytovich frequency $\nu_R = \nu_p\gamma$ is usually given as an estimate to the frequency below which the plasma strongly affects synchrotron radiation. Equation (6) shows that this estimate is not generally valid. We are interested in the regime $(\nu_p/\nu_B)^{1/2} \ll \gamma_e$; hence, for plasma parameters prevailing in GRB afterglows, the frequency at which the plasma greatly affects the synchrotron radiation is $\nu_{R*} = \nu_p(\nu_p/\nu_B)^{1/2}$. It is simple to show that the definition of the plasma frequency (eq. [1]) implies that $\nu_p^2/\nu_B^2 = \xi_e/2\ell\xi_B$, where $\ell = \ln(\gamma_{e,\max}/\gamma_{e,\min})$. Typically, $\ell \sim 4$. Thus,

$$\nu_{R*} = \nu_p\sqrt{\frac{\nu_p}{\nu_B}} = \nu_p\left(\frac{1}{2\ell}\frac{\xi_e}{\xi_B}\right)^{1/4} . \quad (7)$$

An immediate consequence of equation (7) is that for the effect to be apparent, we must have $\nu_p \gg \nu_B$ (or equivalently, $\xi_e \gg 2\ell\xi_B$). Sazonov (1970) also considered the effects of a relativistic plasma on synchrotron emission. However, he only considered a situation in which $\nu \sim \nu_c \ll \gamma\nu_p$, which led him to infer that negative synchrotron reabsorption is only possible for $\nu_p/\nu_B \gg \gamma_e^2$, or equivalently, if $\xi_e/\xi_B \gtrsim \gamma_e^4$. The result in equation (7) shows that this condition is far too restrictive. However, as is discussed in § 4.2, for the effects to be within the detection range of current radio telescopes, we must have $\xi_e/\xi_B \gtrsim 10^5$.

3.1. *The Razin Suppression*

All the information regarding the response of the plasma to electromagnetic waves (e.g., modes propagating through the plasma, loss and gain, etc.) is contained in the dielectric tensor. Specifically, the strong effect of plasma on synchrotron radiation is a manifestation of the deviation of the refractive index from 1, that is, the nontrivial (i.e., "nonvacuum") structure of the dielectric tensor. The expression derived in the Appendix for the dielectric tensor is not complete, i.e., it does not include self-absorption, since we treat

the magnetic field perturbatively. Unfortunately, obtaining a complete expression for the dielectric tensor requires solving a kinetic equation for the plasma, a process that can be avoided by introducing the method of Einstein coefficients. The application of this method requires that over the length scale of the wave phenomenon (i.e., the wavelength), the absorption does not change the wave characteristics considerably. Indeed, since we do not obtain the dielectric tensor explicitly, we do not know a priori the electromagnetic modes that can propagate through the plasma. We must assume, however, that whatever these modes are, the modifications introduced to the dielectric tensor due to the presence of the plasma are dominated by the deviation of the refractive indices from unity, and not by the absorption, that is,

$$\left|1 - n^{(l)}(\nu)\right| \gg \left|\alpha^{(l)}(\nu)\lambda\right| , \tag{8}$$

where $\lambda = c/\nu$ is the wavelength and l denotes the mode. When the condition in equation (8) is not satisfied, one must use a kinetic-equation approach to self-consistently derive a dispersion relation that incorporates the self-absorption.

Since the refractive index depends on the radiation mode under consideration, we now have to determine the modes relevant to the frequency range we are interested in. Motivated by the insight that in "vacuum," absorption is present and the two transverse modes share the same refractive index (i.e., 1), whereas on the other hand, the result obtained above (see § 2) shows that when absorption is neglected, one obtains a finite $\Delta n^{(l)}$ (see eq. [4]), we conclude that the question of determining the relevant modes is resolved by considering whether the following inequality holds,

$$|n_1(\nu) - n_2(\nu)| \ll \left|\alpha_\nu^{(1,2)}\lambda\right| , \tag{9}$$

where α_ν is the synchrotron self-absorption coefficient and λ is the wavelength of radiation. When the condition in equation (9) is satisfied, the normal waves are linearly polarized along and perpendicular to the projection of the magnetic field on the plane of observation (Ginzburg 1989). We denote these polarizations by $\parallel$ and $\perp$, respectively. The power emitted by a single electron is then given by

$$P_{\perp,\parallel}(\nu,\ \gamma) = \frac{\sqrt{3}e^3 B\sin\chi}{2m_e c^2}\left[1 + \left(\frac{\gamma\nu_p}{\nu}\right)^2\right]^{-1/2}\frac{\nu}{\tilde{\nu}_c} \times \left[\int_{\nu/\tilde{\nu}_c}^{\infty} K_{5/3}(z)\,dz \pm K_{2/3}\left(\frac{\nu}{\tilde{\nu}_c}\right)\right] , \tag{10a}$$

$$\tilde{\nu}_c = \frac{3eB\sin\chi}{4\pi m_e c}\gamma^2\left[1 + \left(\frac{\gamma\nu_p}{\nu}\right)^2\right]^{-3/2} , \tag{10b}$$

where B is the strength of the magnetic field and χ is the pitch angle.

If, however, the condition in equation (9) is not satisfied, one cannot neglect the difference between the refractive indices of the normal modes. We are thus required to consider the two normal modes of the plasma, discussed previously in § 2. The normal modes are (quasi-) transverse and are left- and right-circularly polarized. It can be shown (Ginzburg 1989) that half the total power is "converted" into each circularly polarized normal wave (if we take into account terms up to the order of $1/\gamma$). In this case, the power emitted by a single electron is

$$P^{(1,2)}(\nu,\ \gamma) = \frac{\sqrt{3}e^3 B\sin\chi}{m_e c^2}\left[1 + \gamma^2(1 - n_{1,2}^2)\right]^{-1/2} \times \frac{\nu}{\tilde{\nu}_c}\int_{\nu/\tilde{\nu}_c}^{\infty} K_{5/3}(z)\,dz , \tag{11a}$$

$$\tilde{\nu}_c = \frac{3eB\sin\chi}{4\pi m_e c}\gamma^2\left[1 + \gamma^2(1 - n_{1,2}^2)\right]^{-3/2} . \tag{11b}$$

The polarization of synchrotron emission in plasma is further discussed in § 3.3.

If the frequencies of interest are higher than ν_{R*}, the emission does not differ greatly from the emission in vacuum. However, for frequencies $\nu \lesssim \nu_{R*}$, the emitted power is dramatically suppressed for both polarization regimes. This suppression is usually called the Razin effect.

3.2. *Synchrotron Self-Absorption and the Possibility of Negative Reabsorption*

Our calculation of the synchrotron self-absorption coefficient α_ν implements the Einstein relations between emission and absorption coefficients. These relations relate the emission and absorption coefficients of photons having a specific polarization state, or to put it in terms of the previous section, a specific mode propagating through the plasma, which we denote by l. Hence, the expression for the self-absorption coefficient for a specific mode is (Ginzburg 1989)

$$\alpha_\nu^{(l)} = -\frac{c^2}{4\pi\nu^2}\int E^2\frac{d}{dE}\left[\frac{n_e(E)}{E^2}\right]P^{(l)}(\nu,\ E)\,dE , \tag{12}$$

where $P^{(l)}(\nu,\ E)$ is the power of l-polarized photons emitted by an electron with energy E.

Negative contributions to reabsorption come only from regions where the electron distribution function grows faster than E^2. Indeed, if the distribution function has regions that are "steep" enough, the self-absorption coefficient becomes negative at low frequencies ($\nu \lesssim \nu_{R*}$). This corresponds to stimulated emission from the plasma, and radiation is coherently amplified as it propagates. For this reason, the effect is sometimes known as a "maser" effect.

In order to estimate the "amplitude" of the negative self-absorption, we take the electron distribution to be monoenergetic. Substituting $n_e(E) = n_e\delta(E - E_0)$ in equation (12) and using the fact that we are interested in frequencies $\nu \ll \gamma_e\nu_p$, it can be shown that

$$\alpha_\nu \simeq 2\times 10^{-2}\frac{\nu_p\nu_B}{c\sqrt{\gamma_e}\nu}\Phi(Z(\nu)) , \tag{13}$$

where $\Phi(Z) = 2Z\int_Z^\infty K_{5/3}(y)\,dy - 2ZK_{5/3}(Z)$ and $Z(\nu) = (2/3)(\nu_p^3/\nu_B\nu^2)$. The function $\Phi(Z(\nu))$ has a global minimum at approximately $\nu_{R*} = \nu_p(\nu_p/\nu_B)^{1/2}$, and its minimal value is -0.24. Substituting $\nu \sim \nu_{R*}$, we obtain an estimate of the minimal value of the synchrotron self-absorption,

$$\min\alpha_\nu \approx -\frac{10^{-2}}{c\sqrt{\gamma_e}}\nu_B\sqrt{\frac{\nu_B}{\nu_p}} , \tag{14}$$

up to a factor of the order of unity.

3.3. *Polarization of Synchrotron Radiation in Plasma*

We can now use the estimate of the absorption coefficient obtained above to check the self-consistency of our calculation. Namely, we show that in the frequency range of interest, the deviation from unity of the refractive indices dominates the absorption, thus facilitating the validity of implementation of the Einstein-coefficient method, as required by the consistency condition in equation (8). In § A1 we show that the refractive indices can be approximated by $n \approx 1 - (1/2)(\nu_p/\nu)^2$. Hence, for δ-function distributions, equation (8) can be rewritten as $10^2\gamma_e^{1/2}\nu_p^{5/3}/\nu_B^{3/2} \gg \nu$. Since we are interested in frequencies of the order of $\nu_{R*} \sim \nu_p(\nu_p/\nu_B)^{1/2}$, this condition is casted to $10^2\gamma_e^{1/2}\nu_p/\nu_B \gg 1$, which is always satisfied for typical afterglow parameters ($\gamma_e \sim 10^3$, $\nu_p/\nu_B \sim 10^3$).

Next we determine the polarization of the synchrotron modes in the frequency range of interest for us. We use the estimate in equation (4) for Δn and substitute equation (14) for the right-hand side of the inequality in equation (9) with negative reabsorption. After some algebra, we find that the condition in equation (9) is only satisfied for radiation propagating almost perpendicular to the magnetic field, $|\pi/2 - \phi| < 0.1(\nu_B/\nu_p)^{1/2}$, given that $\nu_B/\nu_p \ll 0.02\gamma_e^{-1/2}$. For typical plasma parameters ($\gamma_e \sim 10^3$–10^4, $\nu_p/\nu_B \sim 10^3$), this inequality is not satisfied, and we conclude that the plasma is not isotropic; hence, the normal waves at frequencies $\nu \sim \nu_{R*}$ are circularly polarized.

4. APPLICATION TO GRBs

This section is dedicated to the study of the application of the results obtained above to the plasma conditions prevailing in GRB afterglows. We briefly review the fireball model and obtain the physical parameters of the plasma during the onset of fireball deceleration, considering both expansion into a uniform density ISM (§ 4.1.1) and into a wind (§ 4.1.2). These parameters enable order-of-magnitude estimates of relevant frequencies (§§ 4.2.1 and 4.2.2). We then make a short excursion, referring to the issue of the origin of negative reabsorption in relation to the shape of the electron distribution function at low energies (§ 4.2.3), and conclude the section with a numerical calculation of the resulting spectrum for various electron distribution functions (§ 4.2.4).

4.1. *Fireball Plasma Parameters during the Onset of Deceleration*

According to the fireball paradigm (Paczyński 1986; Goodman 1986), an energetic explosion ($E \sim 10^{51}$–10^{53} ergs) drives a relativistic blast wave into an ambient gas (the "forward shock"). The expanding shell of accelerated ambient gas gradually approaches a self-similar behavior (Blandford & McKee 1976). During the short transition period before self-similarity is established, the interaction between the ejecta and the surrounding medium drives a relativistic shock into the ejecta (the "reverse shock") (Mészáros & Rees 1997) and heats it. The transition to self-similarity occurs on a timescale comparable to the time it takes the reverse shock to cross the ejecta (e.g., Waxman & Draine 2000). The observed radiation is the consequence of synchrotron emission by relativistic shock-accelerated electrons, which gyrate in the magnetic fields generated by the shocks.

Recent data support GRB models in which the outflow is a jet (rather than a sphere), with an opening angle $\theta_{jet} \sim 0.1$ (Waxman, Kulkarni, & Frail 1998; Fruchter et al. 1999; Stanek et al. 1999; Harrison et al. 1999; see Frail et al. 2001 for an update analysis). The dynamics and resulting light curves of such models differ from those of isotropic expansion models after the jet Lorentz factor decreases below $1/\theta_{jet}$. Typically, this happens several hours after the main GRB. We, however, are interested in very early stages of the expansion (typically ~10 s after the main GRB), and so the analysis we present below, although formulated in terms of an isotropic model, is also valid for a jetted scenario.

4.1.1. *Expansion into a Uniform-Density ISM*

Self-similarity is established once the reverse shock crosses the ejecta. It has been shown (Waxman & Draine 2000) that at this time, both the shocked ISM and the heated ejecta propagate with a Lorentz factor that is close to that given by the Blandford-McKee self-similar solution,

$$\Gamma^{(R)} \simeq \Gamma^{(F)} \simeq \left(\frac{17E}{1024\pi n m_p c^5 T^3}\right)^{1/8} = 184 E_{52}^{1/8} n_0^{-1/8} T_1^{-3/8}\,, \quad (15)$$

where $T = 10T_1$ s is the observed burst duration, which is typically of the order of 10 s, $E = 10^{52}E_{52}$ ergs is the explosion energy, and $n = 1n_0$ cm^{-3} is the density of the ambient gas. Accordingly, the electron number density behind the forward shock is

$$n_e'^{(F)} = 4\Gamma^{(F)} n = 735 E_{52}^{1/8} T_1^{-3/8} n_0^{7/8}\ \text{cm}^{-3} \quad (16)$$

(where the prime denotes that this is a quantity measured in the frame comoving with the plasma).

Let $\gamma_p^{(F)}$ and $\gamma_p^{(R)}$ be the Lorentz factors associated with the thermal motion of the protons accelerated by the forward and reverse shocks, respectively. Then it can be shown (Waxman & Draine 2000) that $\gamma_p^{(F)} \simeq \gamma_p^{(R)}\Gamma^2/\Gamma_i$, where $\Gamma_i \sim 300$ is the Lorentz factor of the ejecta prior to its deceleration by the ambient gas (and after the production of the main GRB). This result holds for both relativistic and nonrelativistic reverse shocks. Since the plasmas behind the forward and reverse shocks are separated by a contact discontinuity, the energy densities in the two plasmas are similar. Consequently, we obtain

$$n_e'^{(R)} \simeq \frac{\Gamma^2}{\Gamma_i} n_e'^{(F)} = 8.27 \times 10^4 E_{52}^{3/8} T_1^{-9/8} n_0^{5/8} \Gamma_{i,2.5}^{-1}\ \text{cm}^{-3}\,. \quad (17)$$

Lacking a fundamental theory of Fermi acceleration and formation of magnetic fields by shocks, it is customary to parameterize the fractions of the energy carried by the magnetic field and the electrons by two dimensionless parameters, ξ_B and ξ_e, respectively. We assume that the values of these parameters are similar in the plasmas accelerated by the forward and reverse shocks, as we expect them to be associated with "microphysics" processes in the plasma. Since energy densities behind both shocks are similar, we then have

$$B^{(R)} \simeq B^{(F)} = 0.07\left(\frac{\xi_B}{10^{-6}}\right)^{1/2} E_{52}^{1/8} T_1^{-3/8} n_0^{3/8}\ \text{G}\,, \quad (18)$$

where we use the normalization $(\xi_B/10^{-6})$ since we expect

strong collective plasma effects for small values of ξ_B (see § 1).

Relativistic shock waves are assumed to accelerate protons and electrons to high energies, giving power-law distribution functions

$$n'_e(\gamma) = K\gamma^{-p}, \text{ for } \gamma_{e,\min} < \gamma < \gamma_{e,\max} . \quad (19)$$

Spectral indices $p \gtrsim 2$ were observed in the cosmic-ray spectrum and supernovae radio emission, observations that were later explained by theoretical work (Blandford & Eichler 1987). Numeric and analytic calculations of particle acceleration via the first-order Fermi mechanism in relativistic shocks yield spectral indices $p \approx 2.2$ for highly relativistic shocks (Bednarz & Ostrowski 1998). This result is in agreement with the value of p inferred from GRB afterglow observations (Waxman 1997a, 1997b). The maximum Lorentz factor $\gamma_{e,\max}$ is determined by requiring that the most energetic electrons lose energy through synchrotron emission slower than they gain energy through acceleration by the shock. Normalization then implies

$$\gamma^{e(F)}_{e,\min} = \frac{1}{\ell}\xi_e \frac{m_p}{m_e}\Gamma = 4.22\times 10^4 \ell_4^{-1}\left(\frac{\xi_e}{0.5}\right) E_{52}^{1/8} T_1^{-3/8} n_0^{1/8} , \quad (20)$$

where $\ell = \ln(\gamma_{e,\max}/\gamma_{e,\min})$. Typically, $\ell \sim 4$. Following the discussion leading to equation (16), we have $\gamma^{e(R)}_{e,\min} \simeq \gamma^{e(F)}_{e,\min}\Gamma_i/\Gamma^2$.

4.1.2. *Expansion into a Wind*

We examine here the simplest model of a "wind," in which the star loses mass at a constant rate $\dot{M}$ during an epoch prior to the explosion. Material is ejected radially at a constant speed v, hence producing a nonhomogeneous ambient gas with $n \propto r^{-2}$. Using typical estimates for the mass-loss rate $\dot{M} = 10^{-5}\ M_\odot\ \mathrm{yr}^{-1}$ and for the wind velocity $v = 10^3$ km s^{-1} (Chevalier & Li 1999), one obtains $n = \dot{M}/4\pi m_p v r^{-2} \simeq 3\times 10^{35}(\dot{M}_{-5}/v_3) r^{-2}$ cm^{-3}; here we use the notations $\dot{M}_{-5} = \dot{M}/(10^5\ M_\odot\ \mathrm{yr}^{-1})$ and $v_3 = v/(10^3$ km s$^{-1})$. Once the dynamics reach the self-similar regime, the Lorentz factor and the radius are related through $E = (16\pi/9) m_p c^2 r^3 n(r) \Gamma^2_{\text{B-M}} = (4\dot{M}c^2/9v)\Gamma^2_{\text{B-M}} r$. The physical parameters of the plasmas heated by the forward and reverse shocks are obtained following the reasoning employed in § 4.1.1, and so, without further ado:

$$n'^{(F)}_e \simeq 1.09\times 10^7 E_{52}^{-3/4}\left(\frac{\dot{M}_{-5}}{v_3}\right)^{7/4} T_1^{-5/4}\ \mathrm{cm}^{-3} , \quad (21)$$

$$n'^{(R)}_e \simeq 6.56\times 10^7 E_{52}^{-1/4}\left(\frac{\dot{M}_{-5}}{v_3}\right)^{5/4} T_1^{-7/4}\Gamma_{i,2.5}^{-1}\ \mathrm{cm}^{-3} , \quad (22)$$

$$B^{(R)} \simeq B^{(F)} \simeq 4.18\left(\frac{\xi_B}{10^{-6}}\right)^{1/2} E_{52}^{-1/4} \times \left(\frac{\dot{M}_{-5}}{v_3}\right)^{3/4} T_1^{-3/4}\ \mathrm{G} , \quad (23)$$

$$\gamma^{e(F)}_{e,\min} \simeq 9.78\times 10^3 \ell_4^{-1}\left(\frac{\xi_e}{0.5}\right) E_{52}^{1/4}\left(\frac{\dot{M}_{-5}}{v_3}\right)^{-1/4} T_1^{-1/4} , \quad (24)$$

$$\gamma^{e(R)}_{e,\min} \simeq 1.61\times 10^3 \ell_4^{-1}\left(\frac{\xi_e}{0.5}\right) E_{52}^{-1/4} \times \left(\frac{\dot{M}_{-5}}{v_3}\right)^{1/4} T_1^{1/4}\Gamma_{i,2.5} . \quad (25)$$

4.2. *Razin Cutoff and Synchrotron Maser*

We now use the lessons of the previous three sections to estimate ν_p, ν_B, and ν_c (the synchrotron characteristic frequency) and $\nu_{\mathrm{R}*}$ for the four cases under study, i.e., the ejecta heated by the reverse shock and the ambient medium heated by the forward shock in the two fireball expansion scenarios.

4.2.1. *Expansion into a Uniform-Density ISM*

The typical Lorentz factor of the ISM accelerated by the forward shock is very high, $\gamma^{e(F)}_{e,\min} \simeq 4.2\times 10^4$, and the number density is $n'^{(F)}_e \simeq 735$ cm^{-3}. Under the assumption of a small ξ_B, the magnetic field is $B \simeq 0.07$ G. The values just stated correspond to the epoch of transition to self-similar behavior. Using the results of the last section and boosting to the observer frame (multiplying by Γ), we obtain

$$\nu^{(F)}_p \simeq 2.2\times 10^5 \ell_4^{1/2}\left(\frac{\xi_e}{0.5}\right)^{-1/2} E_{52}^{1/8} T_1^{-3/8} n_0^{3/8}\ \mathrm{Hz} ,$$

$$\nu_B \simeq 870\ell_4\left(\frac{\xi_e}{0.5}\right)^{-1}\left(\frac{\xi_B}{10^{-6}}\right)^{1/2} E_{52}^{1/8} T_1^{-3/8} n_0^{-1/8}\ \mathrm{Hz} ,$$

$$\nu^{(F)}_c \simeq 9.8\times 10^{16}\ell_4^{-2}\left(\frac{\xi_e}{0.5}\right)^{2}\left(\frac{\xi_B}{10^{-6}}\right)^{1/2} E_{52}^{1/2} T_1^{-3/2}\ \mathrm{Hz} ,$$

$$\nu^{(F)}_{\mathrm{R}*} \simeq 3.5\times 10^6 \ell_4^{1/4}\left(\frac{\xi_e}{0.5}\right)^{-1/4}\left(\frac{\xi_B}{10^{-6}}\right)^{-1/4} \times E_{52}^{1/8} T_1^{-3/8} n_0^{3/8}\ \mathrm{Hz} . \quad (26)$$

Since $\gamma^{(F)}_{e,\min}$, B, and $n'^{(F)}_e$ are proportional to $\Gamma \propto r^{-3/2}$, we find that (in the observer's frame) ν_p, ν_B, and $\nu_{\mathrm{R}*} \propto r^{-3/2}$, whereas $\nu_c \propto r^{-6}$.

The ejecta heated by the reverse shock is characterized by a lower Lorentz factor $\gamma^{e(R)}_{e,\min} \simeq 375$, but the number density is much higher than behind the forward shock, $n'^{(R)}_e \simeq 8.3\times 10^4$ cm^{-3}. In the observer's frame,

$$\nu^{(R)}_p \simeq 2.5\times 10^7 \ell_4^{1/2}\left(\frac{\xi_e}{0.5}\right)^{-1/2} E_{52}^{3/8} T_1^{-9/8} n_0^{1/8}\Gamma_{i,2.5}^{-1}\ \mathrm{Hz} ,$$

$$\nu^{(R)}_B \simeq 9.8\times 10^4 \ell_4\left(\frac{\xi_e}{0.5}\right)^{-1}\left(\frac{\xi_B}{10^{-6}}\right)^{1/2} \times E_{52}^{3/8} T_1^{-9/8} n_0^{1/8}\Gamma_{i,2.5}^{-1}\ \mathrm{Hz} ,$$

$$\nu^{(R)}_c \simeq 7.7\times 10^{12}\ell_4^{-2}\left(\frac{\xi_e}{0.5}\right)^{2}\left(\frac{\xi_B}{10^{-6}}\right)^{1/2} n_0^{1/2}\Gamma_{i,2.5}^{2}\ \mathrm{Hz} ,$$

$$\nu^{(R)}_{\mathrm{R}*} \simeq 3.9\times 10^8 \ell_4^{1/4}\left(\frac{\xi_e}{0.5}\right)^{-1/4}\left(\frac{\xi_B}{10^{-6}}\right)^{-1/4} \times E_{52}^{3/8} T_1^{-9/8} n_0^{1/8}\Gamma_{i,2.5}^{-1}\ \mathrm{Hz} . \quad (27)$$

4.2.2. *Expansion into a Wind*

While the reverse shock crosses the ejecta, the heated wind particles are accelerated by the forward shock to a typ-

ical Lorentz factor $\gamma_{e,\min}^{e(F)} \simeq 9.8 \times 10^3$. At that time, the number density is $n_e^{\prime(F)} \simeq 1.1 \times 10^7$ cm^{-3} and the magnetic field is $B \simeq 4.2$ G. Then,

$$\nu_p^{(F)} \simeq 1.3 \times 10^7 \ell_4^{1/2} \left(\frac{\xi_e}{0.5}\right)^{-1/2} \times \left(\frac{\dot{M}_{-5}}{v_3}\right)^{3/4} E_{52}^{-1/4} T_1^{-3/4} \text{ Hz} ,$$

$$\nu_B^{(F)} \simeq 5.1 \times 10^4 \ell_4 \left(\frac{\xi_e}{0.5}\right)^{-1} \left(\frac{\xi_B}{10^{-6}}\right)^{1/2} \times \left(\frac{\dot{M}_{-5}}{v_3}\right)^{3/4} E_{52}^{-1/4} T_1^{-3/4} \text{ Hz} ,$$

$$\nu_c^{(F)} \simeq 7.1 \times 10^{16} \ell_4^{-2} \left(\frac{\xi_e}{0.5}\right)^{2} \left(\frac{\xi_B}{10^{-6}}\right)^{1/2} E_{52}^{1/2} T_1^{-3/2} \text{ Hz} ,$$

$$\nu_{\text{R}*}^{(F)} \simeq 2.0 \times 10^8 \ell_4^{1/4} \left(\frac{\xi_e}{0.5}\right)^{-1/4} \left(\frac{\xi_B}{10^{-6}}\right)^{-1/4} \times \left(\frac{\dot{M}_{-5}}{v_3}\right)^{3/4} E_{52}^{-1/4} T_1^{-3/4} \text{ Hz} . \quad (28)$$

Since during the self-similar stage $n_e^{\prime}$ scales as Γ^5, $B \propto \Gamma^3$, $\gamma_{e,\min} \propto \Gamma$, and $\Gamma \propto r^{-1/2}$, we obtain the following scaling relations for later times: ν_p, ν_B, and $\nu_{\text{R}*} \propto r^{-3/2}$, and $\nu_c \propto r^{-3}$. However, for earlier times, the forward shock expands at a uniform Lorentz factor, and so $\gamma_{e,\min} \propto \Gamma = \text{const}$, $n_e^{\prime} \propto \Gamma n \propto r^{-2}$, and $B \propto (u^{\prime})^{1/2} \propto (\Gamma^2 n)^{1/2} \propto r^{-1}$. Hence, we find that ν_p, ν_B, ν_c, and $\nu_{\text{R}*}$ all scale as r^{-1}.

Finally, the electrons in the ejecta heated by the reverse shock when the fireball expands into a wind have a Lorentz factor of $\gamma_{e,\min}^{e(R)} \simeq 1.6 \times 10^3$ and a number density $n_e^{\prime(R)} \simeq 6.6 \times 10^7$ cm^{-3}. Hence,

$$\nu_p^{(R)} \simeq 7.7 \times 10^7 \ell_4^{1/2} \left(\frac{\xi_e}{0.5}\right)^{-1/2} \left(\frac{\dot{M}_{-5}}{v_3}\right)^{1/4} \times E_{52}^{1/4} T_1^{-5/4} \Gamma_{i,2.5}^{-1} \text{ Hz} ,$$

$$\nu_B^{(R)} \simeq 3.1 \times 10^5 \ell_4 \left(\frac{\xi_e}{0.5}\right)^{-1} \left(\frac{\xi_B}{10^{-6}}\right)^{1/2} \left(\frac{\dot{M}_{-5}}{v_3}\right)^{1/4} \times E_{52}^{1/4} T_1^{-5/4} \Gamma_{i,2.5}^{-1} \text{ Hz} ,$$

$$\nu_c^{(R)} \simeq 2.0 \times 10^{15} \ell_4^{-2} \left(\frac{\xi_e}{0.5}\right)^{2} \left(\frac{\xi_B}{10^{-6}}\right)^{1/2} \left(\frac{\dot{M}_{-5}}{v_3}\right) \times E_{52}^{-1/2} T_1^{-1/2} \Gamma_{i,2.5}^{2} \text{ Hz} ,$$

$$\nu_{\text{R}*}^{(R)} \simeq 1.2 \times 10^9 \ell_4^{1/4} \left(\frac{\xi_e}{0.5}\right)^{-1/4} \left(\frac{\xi_B}{10^{-6}}\right)^{-1/4} \left(\frac{\dot{M}_{-5}}{v_3}\right)^{1/4} \times E_{52}^{1/4} T_1^{-5/4} \Gamma_{i,2.5}^{-1} \text{ Hz} . \quad (29)$$

4.2.3. *The Electron Distribution Function at Low Energies*

As stated in § 3.2, a necessary condition for negative reabsorption is a region that grows faster than E^2 in the electron distribution function. We give here a plausible mechanism that may be responsible for the existence of such a region. Relativistic shock waves are thought to accelerate electrons in such a way that the electron distribution function has a power-law tail extending to high energies. However, there is no satisfactory theory that predicts the shape of the distribution function at low energies. We thus assume that at low energies, the distribution function has the simplest possible behavior, and electrons distribute according to the volume they occupy in phase space, i.e., $n_e(E) \propto E^2$. By emitting synchrotron radiation, the electrons gradually lose their energy and accumulate at lower energies, thus leading to a distribution function that grows faster than E^2 at low energies. The excess of electrons above the E^2 power law is sensitively dependent on the details of the distribution function injected by the shock. Consider, for example, an injected distribution function composed of two *pure* power laws [i.e., $n_e(E) \propto E^2$ if $E \leq E_0$, $n_e(E) \propto E^{-p}$ if $E > E_0$]. This distribution function has a discontinuous derivative at its peak. Synchrotron cooling thus results in an excess of "cooled" electrons just below E_0, leading to a strong maser effect. This issue is treated further in § 4.2.4.

It must be borne in mind, however, that electrons that are "injected" into the hot plasma by the shock at later times have less time to cool. This leads, in principle, to a significant complication in the distribution function of the shock-accelerated electrons, since the farther away from the shock front we look, the "colder" the distribution is, and in general, we cannot consider the distribution function of the shocked plasma to be homogeneous. In particular, in regions closest to the shock front, where the electrons had very little time to cool compared to the dynamical time, the reabsorption is positive, and thus may obscure coherent emission from regions farther away from the shock front. Nevertheless, we have shown numerically that these regions contribute an optical depth of the order of a few, at most, for typical afterglow parameters; hence, the effect of inhomogeneity does not qualitatively change the phenomenon of coherent emission by the relativistic plasma. Furthermore, if one assumes some turbulent mechanism that acts on the dynamical timescale of the system and "mixes" electron populations that were injected by the shock at different times, one can disregard that complication and treat the "averaged distribution" function.

It is interesting to note that a major effect exists even when the low-energy electrons are distributed as $n_e(E) \propto E^2$! Indeed, there is no negative reabsorption in this case, since $\alpha_\nu < 0$ requires a region steeper than E^2 in the distribution function. Nevertheless, the emissivity at $\nu \sim \nu_{\text{R}*}$ is dominated by the low-energy electrons (since j_ν of electrons with $\gamma_e \geq \gamma_{e,\min}$ is Razin-suppressed at higher frequencies). On the other hand, the absorption coefficient, albeit always positive, is dominated by the high-energy electrons and so starts decreasing at frequencies higher than $\nu_{\text{R}*}$. Altogether, we obtain a high peak in the intensity for $\tau_{\nu_{\text{R}*}} \gg 1$ and a strong suppression when $\tau_{\nu_{\text{R}*}} \ll 1$, where $\tau_{\nu_{\text{R}*}}$ is the optical depth at $\nu_{\text{R}*}$.

4.2.4. *Results of Detailed Calculations*

We calculated the emitted intensity for a plasma with $\gamma_{e,\min} = 10^3$–10^4, $\nu_p/\nu_B = 10^2$–10^3. Following the discussion in § 3.3, the normal waves propagating in the plasma are circularly polarized. The intensity of the emitted radiation is given by

$$I_{\nu(1,2)} = j_{\nu(1,2)} \Delta^{\prime} \frac{1 - e^{-\tau_{\nu(1,2)}}}{\tau_{\nu(1,2)}} , \quad (30)$$

where j_ν is the specific emissivity and τ_ν the optical depth.

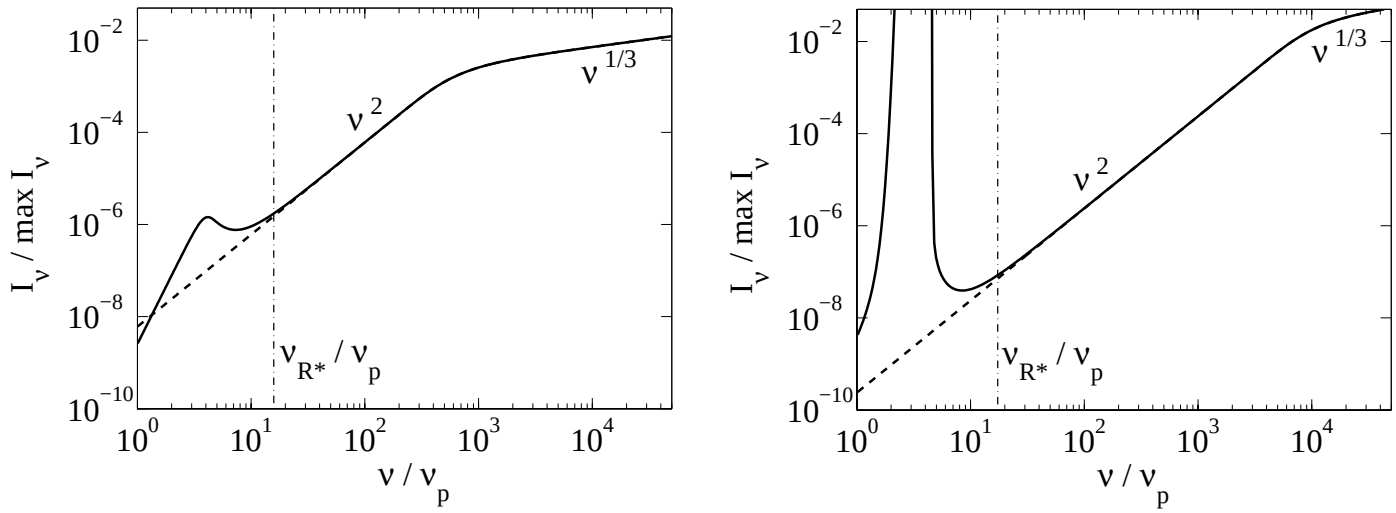

FIG. 1.—Emitted intensity of circularly polarized synchrotron radiation in plasma. Dashed lines represent the "vacuum" values of I_ν, and solid lines represent these quantities when plasma effects are considered. The vertical dash-dotted lines at ν_{R*} separate the region where plasma effects are negligible ($\nu > \nu_{R*}$) from the region where these effects are important ($\nu \lesssim \nu_{R*}$). In order to demonstrate the collective plasma effects given different plasma conditions, two parameter sets were used for the calculations presented here. *Left*: Typical plasma conditions behind a forward shock propagating into a uniform density ISM ($\nu_p \simeq 2 \times 10^5$ Hz in the observer's frame, $\gamma_{e,\min} = 4 \times 10^4$, $n'_e = 10^3$, and $\gamma_{\rm cool}/\gamma_{e,\min} \simeq 2 \times 10^3$). Although there is no negative self-absorption, a $\sim$1.5 order of magnitude increase in the emitted intensity (compared to the emission in vacuum) is apparent at $\nu \lesssim \nu_{R*} \simeq 10^3 \nu_p$ (see § 4.2.3). *Right*: Typical plasma conditions behind a forward shock propagating into a wind ($\nu_p \simeq 10^7$ Hz as measured in the observer's frame, $\gamma_{e,\min} = 10^4$, $n'_e = 10^7$, and $\gamma_{\rm cool}/\gamma_{e,\min} \simeq 10$). The divergence of the emission at $\nu \lesssim \nu_{R*} \simeq 10\nu_p$ is the signature of the maser effect.

The width (as measured in the comoving frame) of the emitting medium along the line of sight Δ' is typically $\sim 10^{13}$ cm in both expansion scenarios.

Using a shock-injected electron distribution function consisting of two pure power laws with typical afterglow parameters, we verified that the cooling scheme suggested in § 4.2.3 results in a maser effect at frequencies $\nu \lesssim \nu_{R*}$. More realistic distribution functions are expected to have a smooth transition region between the two power laws. As an example, we considered the following shock-injected electron distribution function (following Gruzinov & Waxman 1999),

$$n'_e(z) \propto z^2 \left(1 + a z^{-(p+2)}\right)^{-1} , \qquad (31)$$

where $z = \gamma/\gamma_{e,\min}$. The constant a and the overall proportionality factor are chosen such that the distribution is adequately normalized. This distribution function behaves asymptotically as γ^2 at low energies and as γ^{-p} at high energies, with $p = 2.4$. We applied the cooling scheme described in § 4.2.3 to two sets of plasma parameters: one with $\nu_p/\nu_B = 250$, $\gamma_{e,\min} = 4 \times 10^4$, $n'_e = 10^3$ cm^{-3}, and $\gamma_{\rm cool}/\gamma_{e,\min} \simeq 2 \times 10^3$, and the other with $\nu_p/\nu_B = 250$, $\gamma_{e,\min} = 10^4$, $n'_e = 10^7$ cm^{-3}, and $\gamma_{\rm cool} \simeq 10\gamma_{e,\min}$. Here $\gamma_{\rm cool} = 6\pi m_e c/\sigma_{\rm T} B^2 t'_{\rm dyn}$ is the maximal electron Lorentz factor allowing significant synchrotron losses within the dynamic timescale of the system $t'_{\rm dyn}$. The first parameter set corresponds approximately to the conditions prevailing in the ISM heated by the forward shock, when the fireball expands into a uniform-density ISM, while the other corresponds approximately to the physical conditions in the plasma accelerated by the forward shock, when the fireball expands into a wind. The results of the numerical calculations are displayed in Figure 1. When the first parameter set is used (Fig. 1, *left*), there is no negative reabsorption, since the cooling is not efficient enough. An increase of $\sim$1.5 orders of magnitude in the emitted intensity, compared to the emission in "vacuum," is apparent, as explained in § 4.2.3. On the other hand, the second parameter set, which corresponds to a much lower value of $\gamma_{\rm cool}/\gamma_{e,\min}$ (Fig. 1, *right*), clearly shows the maser effect at frequencies $\nu \lesssim \nu_{R*}$, reflecting the negative self-absorption coefficient due to the efficient synchrotron cooling.

5. DISCUSSION

We have derived a dispersion relation for transverse electromagnetic waves in a weakly magnetized relativistic plasma, assuming the electron and proton distribution functions are isotropic. The frequency range in which we were interested was $\nu_p < \nu \ll \gamma_e \nu_p$. Treating the external weak magnetic field as a perturbation, we have shown that at this frequency range, the normal modes are circularly polarized, having refractive indices that can be approximated by the familiar expression $n^2_{1,2} \simeq 1 - (\nu/\nu_p)^2$, where $\nu_p = [(\nu^{\rm NR}_{pe})^2/\gamma_e + (\nu^{\rm NR}_{pp})^2/\gamma_p]^{1/2}$. We have shown that this result is valid whether the electron distribution is assumed to be a δ-function or a power law. We have also calculated the difference between the two refractive indices (see eq. [4]), obtaining $|\Delta n| \simeq (\nu_p^2 \nu_B/\nu^3) \cos\phi \ln(\nu_p^2/4\nu^2)$ for radiation propagating at an angle $\phi < |\pi/2 - 0.1\nu_B\nu/\nu_p^2|$ with respect to the external magnetic field, and $|\Delta n| \simeq \nu_B^2/2\nu^2$ for radiation propagating at larger angles (i.e., almost perpendicular to the field direction).

We next came to consider the effects of the relativistic plasma on synchrotron emission. We have derived an estimate of the frequency at which the plasma effect on the emission becomes significant:

$$\nu_{R*} \simeq \nu_p \min\left\{\gamma, \sqrt{\frac{\nu_p}{\nu_B}}\right\} . \qquad (32)$$

This result generalizes the familiar Razin frequency $\nu_R = \gamma_e \nu_p$ to a regime where $\nu_p/\nu_B \ll \gamma_e^2$, which is the relevant regime for typical plasma parameters at GRB afterglows; hence, we expect a strong effect of the plasma on the synchrotron emission at $\nu_{R*} = \nu_p(\nu_p/\nu_B)^{1/2}$. Consequently, we found that a necessary condition for the collective plasma effects to be observable is $\nu_p/\nu_B \gg 1$. This ratio was shown to depend only on the ratio of ξ_e to ξ_B and on the width of the distribution function (eq. [7]). Hence, $\xi_e/\xi_B \gg 1$ is a necessary condition for the effects to be observable.

We applied the above results to plasma parameters ($\gamma_e \simeq 10^3$–10^4, $\nu_p/\nu_B \simeq 10^2$–10^3) typical to GRB afterglows and found that for $\xi_B \simeq 10^{-6}$ and ξ_e close to equipartition, the plasma had a decisive effect on the synchrotron emission at radio frequencies during the transition of the fireball dynamics to self-similarity. Two expansion scenarios were considered: (1) a blast wave into a uniform-density ISM with $n_e \simeq 1$ cm^{-3}, in which we expect a collective plasma effect on synchrotron emission from the gas heated by the forward shock at $\sim$3.5 MHz; and (2) expansion into a wind, where the number density decreases as r^{-2}. The number density is $\sim 10^4$ cm^{-3} at the radius at which the dynamics become self-similar. In this case, we predict a plasma effect on synchrotron emission from the wind accelerated by the forward shock at $\sim$0.2 GHz (see eqs. [26]–[29]).

Note that collective plasma effects on synchrotron emission below ν_{R*} are expected irrespective of the details of the electron distribution function. This is in contrast to negative reabsorption and the maser effect, which require a region in the electron distribution function that rises faster than E^2. The energy distribution of electrons produced by collisionless shock acceleration is not well known, in particular at low energy. However, we have shown that for plausible assumptions about the electron distribution function at low energy, synchrotron cooling of the electrons may lead to negative reabsorption. This, however, depends on the details of the distribution function near its peak. We have demonstrated negative reabsorption for a distribution that transforms smoothly (at $\gamma_{e,\min}$) from an E^2 power law at low energies to an E^{-p} ($p = 2.4$) power law at high energies, for a certain range of parameters (Fig. 1, *right*).

One should note, however, that even if the distribution function permits negative reabsorption, coherent emission from plasma accelerated by a reverse shock may be completely obscured by the high optical depth of the ambient medium heated by the forward shock. Thus, for example, when the fireball expands into a wind, certain electron distribution functions may lead to coherent emission from the reverse shock at 1.2 GHz (eq. [29]). Nevertheless, the maser due to the reverse shock is completely suppressed by the $\sim 10^3$ optical depth of the forward shock at the GHz frequency range. A similar situation also occurs when the fireball expands into a uniform-density ISM. Note, however, that if turbulent processes disrupt the shock fronts, so that "bulges" of accelerated ejecta lie in front of the forward shell along the line of sight, the plasma effects occurring in the reverse shock may become observable.

Our calculations of coherent emission assumed a homogeneous distribution function in the emitting shell. However, we have numerically shown that even if inhomogeneity due to different cooling times is taken into account, coherent emission would still be observable: the regions close to the shock front, where the electrons have little time to cool, only contribute a positive optical depth of the order of a few and hence do not completely obscure the maser emission from regions farther away from the shock front.

We have shown that for typical plasma parameters, the normal waves propagating in the plasma are circularly polarized at frequencies of the order of ν_{R*} (see the discussion following eq. [9] and § 3.3). Since the difference between the refractive indices of the transverse normal modes is smaller by a factor of $\sim \nu_B/\nu \ll 1$ than $1 - n_{1,2}(\nu)$, and it is the latter that enters the equations of reabsorption and determines the amplification of radiation in both polarizations, the resulting optical depths corresponding to radiation in the two polarizations differ by a factor of a few, at most, if the magnetic field is assumed to be constant throughout the emitting shell. This factor is expected to reduce because of saturation of emitted radiation. If, however, the direction of the magnetic field is assumed to fluctuate randomly on length scales smaller than the shell's width, the difference between the two refractive indices also changes signs randomly, and the difference in the amplifications of the two polarizations is averaged out. Consequently, we do not expect the observed radiation to have a high degree of circular polarization at relevant frequencies.

A detection of a strong effect in the radio band at early stages of the afterglow will place a new independent constraint on the value of ξ_B, as it will prove that it must be much smaller than 1. Since there is a 2 order of magnitude difference between our estimates of ν_{R*} in the forward shock in the two expansion scenarios, a flash in the radio wave band during early afterglow stages seems more probable when the fireball expands into a wind. In this respect, collective plasma effects may serve as an important clue to the GRB environment and progenitor type.

E. W. is the incumbent of the Beracha Foundation career development chair.

APPENDIX

DISPERSION RELATIONS OF TRANSVERSE ELECTROMAGNETIC WAVES IN A RELATIVISTIC PLASMA

Since the rate of binary collisions is much smaller than the frequencies of interest for us, the plasma can be adequately described by a collisionless Vlasov equation,

$$\frac{\partial f_\alpha}{\partial t} + \frac{\boldsymbol{p}}{\gamma m_\alpha} \cdot \nabla f_\alpha + q_\alpha \left(\boldsymbol{E} + \frac{\boldsymbol{p} \times \boldsymbol{B}}{\gamma m_\alpha c} \right) \cdot \frac{\partial f_\alpha}{\partial \boldsymbol{p}} = 0 \,, \tag{A1}$$

where the one-particle distribution function $f_\alpha(\boldsymbol{x}_\alpha, \boldsymbol{p}_\alpha, t)$ is defined as the fractional density of particles of a single type in phase space, and α denotes a single species of particles, i.e., electrons or protons.

A1. TRANSVERSE ELECTROMAGNETIC WAVES IN A FIELD-FREE PLASMA

Let $f_{\alpha 0}$ be an equilibrium distribution function, and let $f_{\alpha 1}(\boldsymbol{x},\ \boldsymbol{p},\ t)$ be a small perturbation to it, so that $f_\alpha = f_{\alpha 0} + f_{\alpha 1}$. It is assumed that the equilibrium distribution function carries no net charge or current distributions. Since we assume that $|f_{\alpha 1}| \ll f_{\alpha 0}$, equation (A1) can be linearized, and we obtain the (Fourier-transformed) perturbation to the equilibrium distribution function

$$f_{\alpha 1} = q_\alpha \frac{\boldsymbol{E} \cdot (\partial f_{\alpha 0}/\partial \boldsymbol{p})}{i(\omega - \boldsymbol{k} \cdot \boldsymbol{p}/\gamma m_\alpha)} \ , \tag{A2}$$

where we have used the assumption that $f_{\alpha 0}$ is isotropic. Here $\omega = 2\pi\nu$. The transverse electromagnetic fields satisfy Maxwell's equations,

$$\begin{aligned} \nabla \times \boldsymbol{E} &= -\frac{1}{c}\frac{\partial \boldsymbol{B}}{\partial t} \ , \\ \nabla \times \boldsymbol{B} &= \frac{1}{c}\frac{\partial \boldsymbol{E}}{\partial t} + \frac{4\pi}{c}\boldsymbol{j} \ , \end{aligned} \tag{A3}$$

where the net current is given by $\boldsymbol{j} = \sum_\alpha \bar{\boldsymbol{n}}_\alpha q_\alpha \int (\boldsymbol{p}/\gamma m_\alpha) f_{\alpha 1}\, d^3p$, the average number density of the particles of the species α is $\bar{\boldsymbol{n}}_\alpha$, and $\gamma = (p^2 + m_\alpha^2 c^2)^{1/2}/m_\alpha c$ is the particle's Lorentz factor. We choose a system of axes such that the radiation propagates with a wavevector $\boldsymbol{k} = (0,\ 0,\ k)$ along the z-axis, whence the transverse electric field is confined to the x-y plane: $\boldsymbol{E} = (E_{\perp 1},\ E_{\perp 2},\ 0)$, and the particle momentum vector is $\boldsymbol{p} = (p_{\perp 1},\ p_{\perp 2},\ p_\parallel)$. Equation (A3) leads to a dispersion relation for the transverse waves,

$$k^2 c^2/\omega^2 E_i = \epsilon_{ij} E_j \quad \text{with } i,\ j = 1,\ 2 \ , \tag{A4}$$

where ϵ_{ij} is the dielectric tensor:

$$\epsilon_{11} = \epsilon_{22} = 1 + \sum_\alpha \frac{(\omega_{p\alpha}^{\rm NR})^2}{\omega} \int d^3p\, \frac{1}{(\omega - k v_\parallel)} \frac{df_{\alpha 0}}{dp} \frac{p_{\perp 1}^2}{p} \frac{m_\alpha c}{\sqrt{p^2 + m_\alpha^2 c^2}} \ , \tag{A5a}$$

$$\epsilon_{12} = -\epsilon_{21} = 0. \tag{A5b}$$

Here $\omega_{p\alpha}^{\rm NR} = (4\pi \bar{\boldsymbol{n}}_\alpha q_\alpha^2/m_\alpha)^{1/2}$ is the nonrelativistic plasma frequency of the species α. The refractive index $n(\omega) = kc/\omega$ for the transverse waves is the square root of the doubly degenerate eigenvalue of equation (A4).

If the electron and proton distribution functions can be approximated by δ-functions $f_{\alpha 0} = (1/4\pi p_{\alpha 0}^2)\delta(p - p_{\alpha 0})$, equation (A5a) becomes

$$\epsilon_{11} = \epsilon_{22} = 1 - \sum_\alpha \frac{(\omega_{p\alpha}^{\rm NR})^2}{2\gamma_{\alpha 0}\omega^2} x_\alpha \left\{ \left[x_\alpha^2 \left(1 - \frac{1}{\gamma_{\alpha 0}^2}\right) - 1 \right] \ln \left| \frac{x_\alpha - 1}{x_\alpha + 1} \right| + 2x_\alpha \left(1 - \frac{1}{\gamma_{\alpha 0}^2}\right) \right\} \ , \tag{A6}$$

with $x_\alpha = \omega/k v_{\alpha 0}$ and $v_{\alpha 0} = p_{\alpha 0}/\gamma_{\alpha 0} m_\alpha$. It can be shown that in the frequency range of interest and for relevant values of $\gamma_{e,p}$, the second term in the curly brackets of equation (A6) dominates the first term for both the electrons and the protons. This can be used to approximate the refractive index by

$$n_{\rm app}^{a2}(\omega) = 1 - \left(\frac{\omega_p}{\omega}\right)^2 \ , \tag{A7a}$$

$$\omega_p = \left(\frac{4\pi \bar{\boldsymbol{n}}_e e^2}{\gamma_{e,0} m_e} + \frac{4\pi \bar{\boldsymbol{n}}_e e^2}{\gamma_{p,0} m_p} \right)^{1/2} = \left[\frac{(\omega_{pe}^{p\rm NR})^2}{\gamma_{e,0}} + \frac{(\omega_{pp}^{p\rm NR})^2}{\gamma_{p,0}} \right]^{1/2} \ . \tag{A7b}$$

Both observations and theory imply that in afterglow plasmas, the electrons are not distributed monoenergetically, but rather have a distribution function that extends to high energies as a power law, with a spectral index $p \gtrsim 2$. However, we have shown numerically that in the frequency range of interest for us, where $|1 - (kc/\omega)| \gg 1/\gamma_e^2$ and for relevant values of electron and proton Lorentz factors, $|1 - n_{\rm PL}|$ differs from $|1 - n_\delta|$ by less than 1 part in 10^4, where n_δ and $n_{\rm PL}$ are the refractive indices for the monoenergetic and power-law distribution functions, respectively. Consequently, the result in equation (A7a) still holds approximately for a power-law distribution. Hereafter, we use δ-function distributions to evaluate the deviation of the refractive index from 1.

A2. TRANSVERSE ELECTROMAGNETIC WAVES IN A WEAKLY MAGNETIZED PLASMA

Let $f_{\alpha 0}$ be an isotropic equilibrium distribution function, which describes a plasma in an external uniform magnetic field $\boldsymbol{B}_0$. We introduce a small perturbation to $f_{\alpha 0}$. Since we are interested in frequencies $\omega \gg \omega_B$, we assume that the external magnetic field is small, so that the perturbation is made up of two contributions, one (which we denote by $f_{\alpha 1}$) that is independent of the magnetic field, and another (denoted by $f_{\alpha 2}$) that is linear in the magnetic field; thus, $f_{\alpha 0} \gg |f_{\alpha 1}| \gg |f_{\alpha 2}|$. We now linearize the Vlasov equation (see eq. [A1]) and neglect $(\partial f_{\alpha 2}/\partial \boldsymbol{p})$ with respect to $(\partial f_{\alpha 1}/\partial \boldsymbol{p})$. Substituting equation (A2) for $f_{\alpha 1}$, we obtain

(after some algebra)

$$f_{\alpha 2} = -\frac{q_\alpha^2}{\gamma m_\alpha c}\frac{(df_{\alpha 0}/dp)}{p}(\boldsymbol{p}\times\boldsymbol{B}_0)\cdot\left[\frac{\boldsymbol{E}}{(\omega-\boldsymbol{k}\cdot\boldsymbol{p}/\gamma m_\alpha)^2}+\frac{(\boldsymbol{E}\cdot\boldsymbol{p})\boldsymbol{k}}{\gamma m_\alpha(\omega-\boldsymbol{k}\cdot\boldsymbol{p}/\gamma m_\alpha)^3}\right]. \tag{A8}$$

Hence, $f_{\alpha 2}$ is indeed linear in the external magnetic field, consistent with our assumption.

As already mentioned, we are interested in frequencies $\omega \gg \omega_B$. For these frequencies, the effect of the magnetized plasma on the propagating radiation is small, and the electric field can be assumed to be approximately transverse, i.e., $\boldsymbol{E}\perp\boldsymbol{k}$. Our previous choice of axes is convenient for the analysis; without any loss of generality, we choose $\boldsymbol{B}_0 = (0,\ B_0\sin\phi,\ B_0\cos\phi)$. Following the steps outlined in equations (A3)–(A5a), we obtain the dielectric tensor for quasi-transverse electromagnetic waves in a weakly magnetized plasma,

$$\epsilon_{12} = -\epsilon_{21} = i\sum_\alpha \frac{(\omega_{p\alpha}^{\rm NR})^2}{\omega}\omega_{B\alpha}^{\rm NR}\cos\phi\int d^3p\,\frac{1}{(\omega-kv_\parallel)^2}\frac{df_{\alpha 0}}{dp}\frac{p_{\perp 1}^2}{p}\frac{m_\alpha^2c^2}{p^2+m_\alpha^2c^2}, \tag{A9}$$

with $\omega_{B\alpha}^{\rm NR}\equiv|q_\alpha|B_0/m_\alpha c$ the nonrelativistic gyration frequency. The expression for $\epsilon_{11}=\epsilon_{22}$ is given in equation (A5a). For monoenergetic electron and proton distributions, equation (A9) becomes

$$\epsilon_{12} = -\epsilon_{21} = i\sum_\alpha \frac{(\omega_{p\alpha}^{\rm NR})^2\omega_{B\alpha}^{\rm NR}}{\omega^3}\frac{\cos\phi}{2\gamma_{\alpha 0}^2}x_\alpha^2\left[\left(1-\frac{1}{\gamma_{\alpha 0}^2}\right)x_\alpha\ln\left|\frac{x_\alpha-1}{x_\alpha+1}\right|-\frac{2}{\gamma_{\alpha 0}^2}\frac{1}{x_\alpha^2-1}-2-\frac{10}{\gamma_{\alpha 0}^2}\right], \tag{A10}$$

where x_α has the same definition as in equation (A6).

REFERENCES

Bednarz, J., & Ostrowski, M. 1998, Phys. Rev. Lett., 80, 3911
Blandford, R., & Eichler, D. 1987, Phys. Rep., 154, 1
Blandford, R. D., & McKee, C. F. 1976, Phys. Fluids, 19, 1130
Chevalier, R. A., & Li, Z.-Y. 1999, ApJ, 520, L29
Crusius, A., & Schlickeiser, R. 1988, A&A, 196, 327
Frail, D. A., et al. 2001, ApJ, 562, L55
Fruchter, A. S., et al. 1999, ApJ, 519, L13
Galama, T. J., et al. 1999, Nature, 398, 394
Ginzburg, V. L. 1989, Applications of Electrodynamics in Theoretical Physics and Astrophysics (2d ed.; New York: Gordon & Breach)
Ginzburg, V. L., & Syrovatskii, S. I. 1965, ARA&A, 3, 297
Goodman, J. 1986, ApJ, 308, L47
Gruzinov, A., & Waxman, E. 1999, ApJ, 511, 852
Harrison, F. A., et al. 1999, ApJ, 523, L121
Kulkarni, S. R., et al. 2000, in AIP Conf. Proc. 526, Gamma-Ray Bursts: 5th Huntsville Symp., ed. R. M. Kippen, R. S. Mallozzi, & G. J. Fishman (Melville: AIP), 277
Livio, M., & Waxman, E. 2000, ApJ, 538, 187
MacFadyen, A. I., & Woosley, S. E. 1999, ApJ, 524, 262
Mészáros, P. 2002, ARA&A, 40 , in press (astro-ph/0111170)
Mészáros, P., & Rees, M. J. 1997, ApJ, 476, 232
Paczyński, B. 1986, ApJ, 308, L43
Paczyński, B. 1998, in AIP Conf. Proc. 428, Gamma-Ray Bursts: 4th Huntsville Symp., ed. C. A. Meegan, R. D. Preece, & T. M. Koshut (Woodbury: AIP), 783
Piran, T. 2000, Phys. Rep., 333, 529
Rybicki, G. B., & Lightman, A. P. 1979, Radiation Processes in Astrophysics (New York: Wiley)
Sazonov, V. N. 1969, Soviet Phys.–JETP, 29, 578
———. 1970, Soviet Astron.–AJ, 13, 797
———. 1973, Soviet Astron.–AJ, 16, 971
Smolsky, M. V., & Usov, V. V. 2000, ApJ, 531, 764
Stanek, K. Z., et al. 1999, ApJ, 522, L39
Usov, V. V., & Katz, J. I. 2000, A&A, 364, 655
Waxman, E. 1997a, ApJ, 485, L5
———. 1997b, ApJ, 489, L33
Waxman, E., & Draine, B. T. 2000, ApJ, 537, 796
Waxman, E., Kulkarni, S. R., & Frail, D. A. 1998, ApJ, 497, 288
Waxman, E., & Loeb, A. 1999, ApJ, 515, 721
Wijers, R. A. M. J., & Galama, T. J. 1999, ApJ, 523, 177
Woosley, S. E. 1993, ApJ, 405, 273
Yokun, S. P. 1968, Astron. Lett., 2, 181
Zheleznyakov, V. V. 1967, Soviet Phys.–JETP, 24, 381